MODELLING MECHANICALLY VENTILATED DOUBLE SKIN FACADES WITH INTEGRATED SHADING DEVICE

Alessandro Dama[1], Diego Angeli[2],
[1]Department of Energy, Politecnico di Milano, Milano, Italy
[2]Department of Sciences and Methods for Engineering, Università degli Studi di Modena e Reggio Emilia, Reggio Emilia, Italy

ABSTRACT

Double skin façades (DSF), are typically composed by two transparent envelope elements separated by a ventilated airspace. Such a technology can be applied both in new and existing buildings and may combine architectural value with energy efficiency. In the most common mechanically ventilated configurations the DSF air inlet came from the indoor environment and the outlet air returns to the HVAC system. Integrated shading devices are positioned between the skins.

The assessment of the energy performance of buildings with DSFs requires proper dynamic simulation tools, based on models capable of predicting DSF heat transfer under variable boundary conditions, at the price of a reasonable computational effort.

Many DSF simplified models have been developed and implemented in building simulation tools, but the validation of these tools is still an open issue, especially in presence of shading devices. The CFD modelling activity presented in this work aims at supporting the assessment of a DSF simplified model, specifically developed for the dynamic simulation of heat transfer in buildings. Such a model is based on an integral approach to the vertical channel, which is assumed to be separated into two channels when the shading device is used. Averaged surface heat transfer coefficients, depending on the geometry and flow regime, are adopted in order to represent convection inside the channels, according to the available correlations.

The dataset of a measurement campaign, which was performed in a twin test facility on a mechanically ventilated DSF adopting both Venetian and roller blinds, was used to validate both the CFD model developed for this study, and the implementation of a former simplified model suitable for building simulation. The CFD approach allows for an assessment of the assumptions and hypotheses employed by the simplified model. Moreover, the CFD analyses provide a deeper insight on important aspects such as, the presence and impact of recirculation, the development of velocity and temperature profiles.

INTRODUCTION

The assessment of the energy performance of buildings with Double Skin Facades requires proper dynamic simulation tools, based on models capable of predicting DSF heat transfer under variable boundary conditions, at the price of a reasonable computational effort.

Many DSF simplified models have been developed and implemented in building simulation tools, but the validation of these tools is still an open issue, especially in presence of shading devices. [Tanimoto 1997, Saelens 2002, Zollner at al.2002, Manz 2004, Park 2004, Jiru at al. 2006,] The CFD modelling activity presented in this work aims at supporting the assessment of a simplified model, specifically developed for the integration of DSF component in the building dynamic simulation.

The thermal model is based on an integral approach to the vertical channel, which is assumed to be separated into two channels when the shading device is used. Averaged surface heat transfer coefficients, depending on the geometry and flow regime, are adopted in order to represent convection inside the channels, according to the available correlations.

A former experimental validation of a simplified model was carried out using the dataset of a measurement campaign, which was performed in twin test facades on mechanically ventilated DSF adopting both Venetian and roller blinds. [Angelotti et al. 2007]. The aim of this work is to provide a more detailed assessment of the assumptions and of the hypotheses employed by the simplified model, in order to support its improvement and reliability. For the purpose of a better understanding of the thermo-fluid dynamic phenomena a CFD model was also developed.

The boundary conditions, both for the simplified and the CFD model, are the temperatures of the inlet air and of the surfaces inside the DSF channel. The mass flow rate is given and the validation is based on the prediction of the outlet temperature. In the following Section we describe the experimental case study and the models features and assumptions.

METHODS

Case Study

The experimental case study consist in a Double Skin Façade module mounted in the TWINS test facility of the Department of Energy at Politecnico di Torino, which is detailed described in [Micono at al. 2006].

The DSF module consists of an internal single glass and an external double glass unit, the air gap is ventilated mechanically and has a thickness of about 15 cm. The air circulation is from the indoor environment to the HVAC system. Two alternative shading systems were integrated and tested: Venetian blinds in aluminium with micro-holes tilted at 45° and a reflecting Roller blind in PVC.

The measurements points are shown in Figure 1, they include:

- Thermocouples for inlet, outlet and air temperatures at three heights, both in the internal and external channel
- Thermocouples for the surface temperature of the glazing systems and of the shading device
- Heat flux meters on the glazing surfaces
- A volumetric flow meter.

Table 1
Codes used for the data selected from the measurement campaign

date	hour	Shd. Sys	flow rate	code
June 28, 2005	10:00	Venetian blinds	Low	VL-a
	13:00		Low	VL-b
	16:00		Low	VL-c
June 30, 2005	10:00		High	VH-a
	13:00		High	VH-b
	16:00		High	VH-c
July 26, 2005	10:00	Roller blinds	Medium	RM-a
	13:00		Medium	RM-b
	16:00		Medium	RM-c

Table 2
Experimental data used as boundary condition for the model assessment

code	V'	$T_{air,in}$	T_{glz1}	T_{shd}	T_{glz2}
	m^3/h	°C	°C	°C	°C
VL-a	27.4	30.9	32.9	41.6	40.6
VL-b	27.1	35.4	39.3	52.6	52.6
VL-c	26.7	31.7	35.7	42.6	43.9
VH-a	79.4	27.6	30.4	36.3	36.5
VH-b	79.0	31.4	35.0	44.8	47.3
VH-c	78.6	28.3	32.4	36.7	39.4
RM-a	56.3	28.4	29.7	38.2	36.5
RM-b	56.1	33.1	35.6	48.9	50.9
RM-c	56.5	28.6	31.1	35.9	38.0

For the model assessment carried out in this work, nine operational conditions have been selected from the dataset of the measurement campaign, they are reported in Table 1.

Since the assessment focus on the thermal fluid dynamics in the channel, the boundary conditions chosen to define the problem are the wall temperatures, which in the simplified models are assumed to be uniform. Therefore the glazing and shading surface temperatures at different heights have been averaged. The averaged experimental data are reported in Table 2 (glz1 refers to the external face of the internal glazing, glz2 refers to internal face of the external glazing)

In all the selected operating conditions the ratio Gr/Re^2 induces to considerate a regime of mix convection in both the channel which are created by the interposition of the shading device.

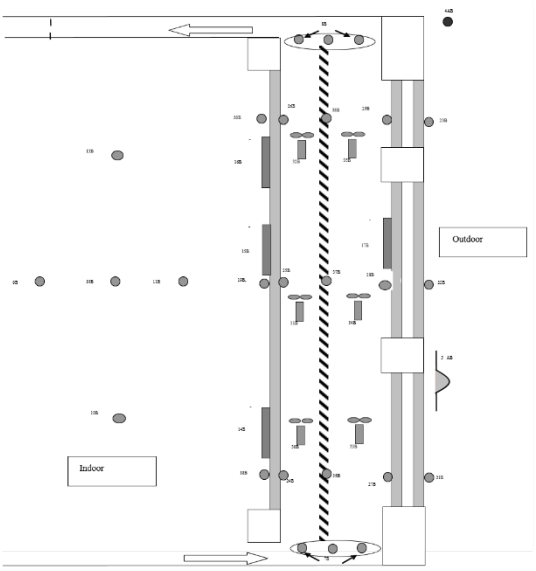

Figure 1:Measurement points in the TWINS test facility at Politecnico di Torino

Model for building simulation

The model here presented (for now on addressed as BS Model) is based on the integration of a mono-dimensional differential formulation of the energy balance proposed in EN 13363-2 [CEN 2005] for ventilated cavities and reported in equation (1).

The main assumptions are uniform wall temperatures (T_w) and uniform convective heat transfer coefficients (h^*_{cv}), which are related to the temperature differences between the surface and the bulk temperature at any height.

$$\begin{cases} [h^*_{cv1}(T_{w1}-T(y))+h^*_{cv2}(T_{w2}-T(y))]Ldy = \dot{m}c_p dT \\ T(0)=T_{in} \quad 0 \le y \le H \end{cases}$$

$$T(y)=\overline{T}_w+(T_{in}-\overline{T}_w)e^{-ky} \qquad \begin{cases} \overline{T}_w \equiv \dfrac{h^*_{cv1}T_{w1}+h^*_{cv2}T_{w2}}{h^*_{cv}+h^*_{cv}} \\ k \equiv \dfrac{(h^*_{cv1}+h^*_{cv2})}{s\,v_m\rho_m c_p} \end{cases} \qquad (1)$$

The corresponding 2D representation of the bulk temperature in the channels is defined in equation (2):

$$T(y) \equiv \frac{1}{s}\int_0^s \rho(x,y)u_y(x,y)T(x,y)dx \qquad (2)$$

In presence of a shading layer the DSF channel is modelled as two parallel ventilated channels, with a flow separation at the inlet (bottom) and a full mixing at the outlet (top), with the assumption that there is no mass flow through the shading layer that separates them and that the volume flow rate is proportional to the thickness of the two channels, *i.e.* the averaged air velocities are equal. This assumptions are obviously *a priori* not justified - especially with Venetian blinds and other permeable shading devices - and will be discussed in the next section.

A key issue in the implementation of the formulation given in (1) is the determination of the convective heat transfer coefficients (h_{cv}).

The correlation for the convective problem proposed in EN 13363-2 combine a correlation for closed cavity with a correction term proportional to the air velocity. As a consequence the convective coefficient depends only by the flow rate and the temperature difference between the walls. It does not take into account the convection driven by the temperature difference between the walls and the inlet air, which can be prevalent when glazing and shading temperatures are both higher or lower the bulk temperatures.

In order to take into account both the effects of the temperature differences between walls and inlet air, the model has been implemented with an algorithm that separates any channel in two sections when the bulk temperature achieve the value of one of the two walls.

According to the experimental boundary condition selected the first section (always with $T_{air} < min(T_{gls}, T_{shd})$) is treated as a wide channel or narrow (respectively according with the criteria $Ra_H^{1/4} > or < H/s$, where H is the height and s the thickness of the ventilated air gap) heated by uniform wall temperatures.

The second section (with $T_{gls} < T_{air} < T_{shd}$ or $T_{shd} < T_{air} < T_{glz}$), when appears, is treated with correlation adapted from closed cavities.

The best suitable correlations for this cases have been selected by an extensive review given in [Saelens 2002] for naturally and mechanically ventilated DSF. They are listed in Table 1.

In any section, Nusselt numbers derived for natural and forced convection are combined according to the following relation:

$$Nu_H^{(mix)} = ((Nu_H^{(for)})^3 + (Nu_H^{(nat)})^3)^{1/3} \qquad (3)$$

Moreover the convective coefficients derived from correlations which are based on the temperature difference between the wall and the inlet air are scaled according to the following relation in order to be used in equation (1).

$$h_{cv}^* = h_{cv}\frac{T_w - T_{in}}{T_w - T_{ave}} \qquad (4)$$

A double iteration loop is necessary to fix the section length and the (volume) averaged bulk temperature. The iterative process is presented in Figure 2.

Table 3
Correlations for convection

LENGHT & ΔT	CASE	AUTHOR
Nu^{for}_H $(T_w\text{-}T_{in})$	Forced (turbulent) convection on vertical walls	Bejan (1984); averaged values are extrapolated from local *Nu*
Nu^{nat}_H $(T_w\text{-}T_{in})$	Natural convection on vertical walls	Churchill & Chu (1975)
$Nu^{nat}{}_s$ $(T_{w1}\text{-}T_{w2})$	Natural convection in closed cavities	ElSherbiny (1982)

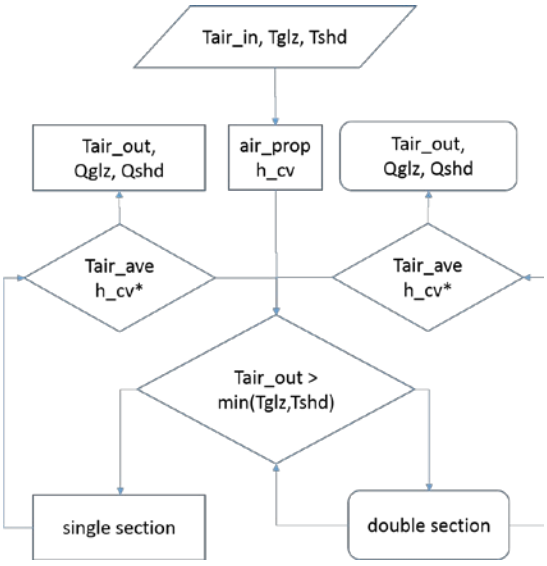

Figure 2: model iteration flow

CFD model

Two-dimensional, steady-state numerical simulations have also been carried out in the frame of the present work, with the twofold purpose of drawing a comparison with the results of the analytical model described above, and of validating the numerical approach itself in light of the experimental benchmark. The calculations are carried out by

means of a finite-volume solver based on the open source OpenFOAM® computational toolbox [Weller et al. 1998], implementing the Reynolds-Averaged Navier-Stokes and energy conservation equations governing non-isothermal, turbulent flow, as well as several turbulence models [Wilcox 2006]. The Oberbeck-Boussinesq approximation has been assumed to be valid, all fluid properties being taken as constant except for density in the buoyancy term. Turbulence has been modelled by means of the SST k-ω model [Menter 1994]. Turbulent heat diffusivity has been determined by means of the Reynolds analogy, assuming a constant value of the turbulent Prandtl number $Pr_t = 0.85$.

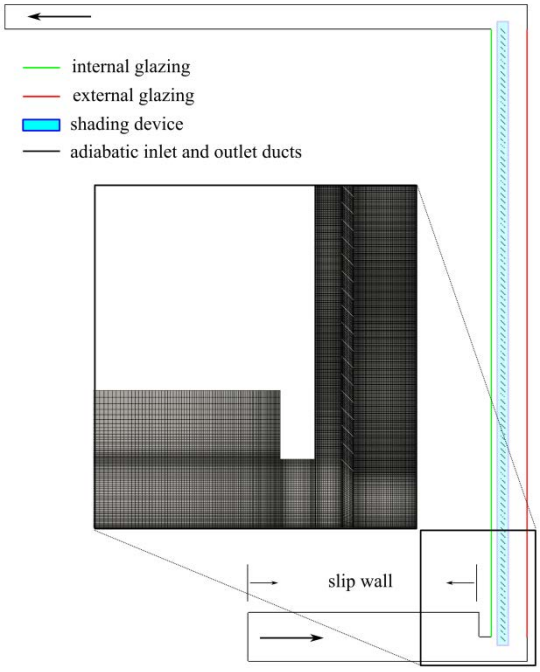

Figure 3 Schematic of the domain for CFD analyses and detail of the computational grid

The 2D computational domain for the simulations is schematized in Figure 3. The shape of the double-skin façade of the TWINS facility has been represented in reasonable detail, based on the available documentation; only the outline of the window framing has not been included in the model, its effect being arguably marginal in the determination of the overall heat transfer. The domain boundaries have been subdivided as reported in Figure 3, and uniform temperature conditions have been imposed at all glazed surfaces of the façade, as well as on the surface of the shading device. Temperature values were directly extrapolated from the experimental data, by averaging the samples collected by different wall-mounted thermocouples (see Figure 1). Hence, the real physics of radiation and of conjugate heat transfer between the glazing and frames and the surrounding air, has been substituted with the assumption of constant wall temperature. Albeit strong, such an approximation is deemed to be sufficiently realistic for the scope of the present work.

A detail of the block-structured computational grid is displayed in Figure 1. The total number of quadrilateral mesh elements amounts to approximately 250000 for both the grids of the roller and venetian blind cases. Near-wall sizing has been chosen so as to avoid the resort to wall functions and, hence, to reproduce the mean features of the diffusive sub-layers. Second-order schemes were adopted for the discretization of both the convective and diffusive terms. The SIMPLE algorithm [Patankar 1980] has been employed for the de-coupling of pressure and velocity.

Table 4
Outlet air temperatures:
BS and CFD models against measurements

Code	T_{out} EXP.	T_{out} BS-model	*errΔT*	T_{out} CFD	*errΔT*
	°C	°C		°C	
VL-a	**37.9**	39.8	*26%*	40.0	*30%*
VL-b	**48.9**	50.4	*12%*	51.0	*16%*
VL-c	**42.9**	41.8	*-10%*	42.2	*-6%*
VH-a	**33.5**	35.2	*29%*	34.9	*24%*
VH-b	**41.9**	43.3	*13%*	43.4	*15%*
VH-c	**37.2**	36.1	*-12%*	36.2	*-11%*
RM-a	**33.4**	35.9	*51%*	35.4	*40%*
RM-b	**45.1**	47.0	*16%*	46.2	*9%*
RM-c	**36.1**	35.4	*-10%*	34.7	*-19%*

RESULTS AND DISCUSSION

The validation of the effectiveness of the BS model is based on the prediction of the outlet air temperature, because this is directly connected with the total heat flux exchanged by convection between the façade walls and the air circulating inside. A comparison between the CFD and BS model predictions with the experimental outlet temperatures is given in Table 4. The discrepancies between predicted and measured values are given in terms of relative errors on the total heat exchanged with air, from the inlet to the outlet, defined in equation (5):

$$errΔT \equiv \frac{T_{out} - T_{out,EXP}}{T_{out,EXP} - T_{in}} \qquad (5)$$

In Table 4 we observe that the differences between the predicted and measured outlet temperatures show a negative trend as the day progresses: they are overestimated at 10 am, while they are underestimated at 4 pm; this happens with all the shading and flow rate configurations and for both the CFD and the BS Model, which show a good

agreement between each other. Such a trend can be due to the effect of the thermal inertia of the DSF frames, which were not modeled, since both the CFD and the BS model assume uniform wall temperatures (set to the averaged values obtained from the measurements on the glass surfaces). This effect should be further addressed for a complete validation of the DSF models. Overall, present results show relative differences below 20% in cases "*b*" and "*c*"; higher discrepancies occur in cases "*a*", when the measured temperature increase along the channel is less relevant.

Table 5
Outlet air temperatures:
BS model against EN 13363-2

Code	T_{out1} EN 13363-2	T_{out1} BS-model	T_{out2} EN 13363-2	T_{out2} BS-model
	°C	°C	°C	°C
VL-a	37.3	37.3	39.8	41.0
VL-b	45.9	45.9	43.9	52.6
VL-c	39.1	39.1	42.1	43.1
VH-a	33.0	32.9	31.2	36.3
VH-b	39.6	39.5	41.1	45.1
VH-c	34.0	34.1	34.9	37.0
RM-a	33.9	33.9	34.9	36.9
RM-b	42.2	42.1	45.6	49.3
RM-c	33.4	33.4	34.8	36.3

Table 6
Convective heat transfer:
EN and BS models against CFD

RM	mod.	Q_{glz1}	Q_{shd1}	Q_{shd2}	Q_{glz2}
		W/m	W/m	W/m	W/m
-a	EN mod	-26.6	49.6	33.2	23.5
	BS-mod	-23.4	46.3	43.1	30.7
	CFD	**-13.9**	**40.7**	**36.9**	**26.7**
-b	EN mod	-49.3	86.7	47.3	59.3
	BS-mod	-42.5	79.7	61.2	76.8
	CFD	**-32.4**	**64.6**	**59.9**	**78.7**
-c	EN mod	-7.4	27.6	21.1	33.2
	BS-mod	-6.1	26.3	26.7	41.2
	CFD	**-3.5**	**23.9**	**22.5**	**36.6**

A comparison between the outlet temperatures of each separated channel predicted employing EN 13363-2 standard instead of the correlations adopted in the BS model is reported in Table 5. In the first channel the model results are very close, while in the second channel EN13363-2 generally underestimates heat transfer; this in due to the fact it does not take into account the convection driven by the temperature difference between the wall and the inlet air.

A further comparison between the predictions of the EN and BS models and CFD results is brought forth in Table 6, in terms of global heat transfer at all active walls, for the cases with roller blinds. It is observed that the BS-model agrees better with CFD than the EN model in the case where temperature gradients become more significant (cases "*b*").

Figure 4 reports an overall view of the flow and thermal fields in three of the nine configurations investigated here. With reference to Table 1, these configurations are representative of a case with venetian blinds and a low flow rate (VL-b, Figure 4a), a case with venetian blinds and a high flow rate , (VH-b, Figure 4b) and a case with a roller blind (RM-b, Figure-4c). Temperature and vertical velocity profiles are also reported in Figure 5 for the same cases, sampled at selected heights along the façade, corresponding to the locations where monitoring thermocouples were installed in the facility (see also Figure 1).

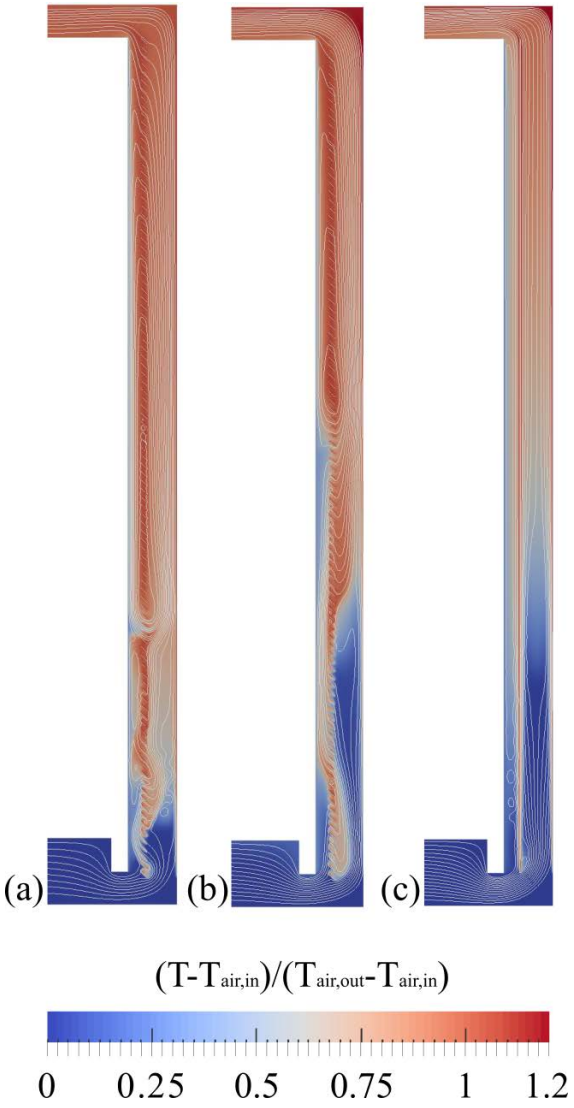

Figure 4 Normalized temperature maps and streamlines from CFD: (a) VL-b; (b) VH-b; (c) RM-b

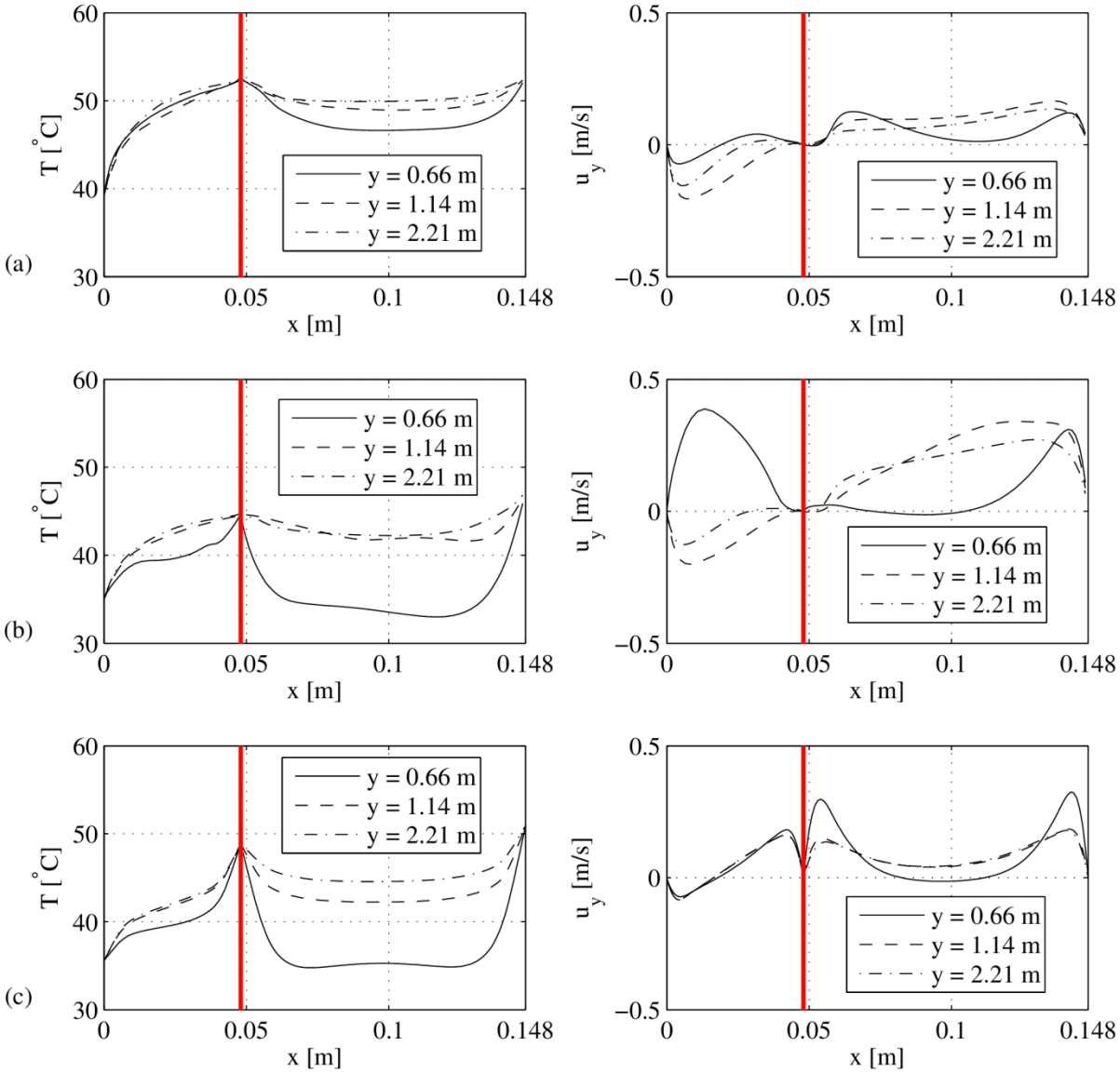

Figure 5 Temperature (left) and vertical velocity (right) profiles at selected heights, corresponding to the locations of thermocouple rakes in the TWINS facility: (a) case VL-b; (b) case VH-b; (c) case RM-b.

Although different patterns are observed, depending on the geometry and boundary conditions, some common features could be indeed singled out. Due to the specific layout of the entrance region, a major part of the flow rate is directed towards the external channel. In contrast, large recirculation regions are always predicted in the internal channel, as a result of the weaker inertia of the flow, and of the strong density gradients produced by the considerable temperature difference which invariably establishes between the shading device and the internal glass. Hence, flow in a large part of the internal channel exhibits the typical characteristics of cavity flow. This is particularly evident when looking at the case with roller blinds (Figures 4c and 5c), where the two channels are physically separated for the whole height of the façade. A large recirculation bubble elongates from the bottom to the top of the internal channel, creating a downward flow along the internal glass, and a slightly stronger upward stream along the roller screen, enhanced by the feeble inertial component. As a result, velocity profiles at different heights are almost overlapping in the internal channel, while temperature profiles are typical of those occurring in a vertical slot. On the other hand, in the external channel, two distinct boundary layers form along the roller and external glass, and progressively merge in a single channel-like flow as the fluid mean temperature rises with height. Such characteristics appear to be consistent with the modelling choices adopted to represent buoyancy-induced heat transfer in the BS model.

In the cases with venetian blinds, the horizontal extent of the recirculation region encompasses also part of the external channel, due to the processes of mass transfer through the blind itself.

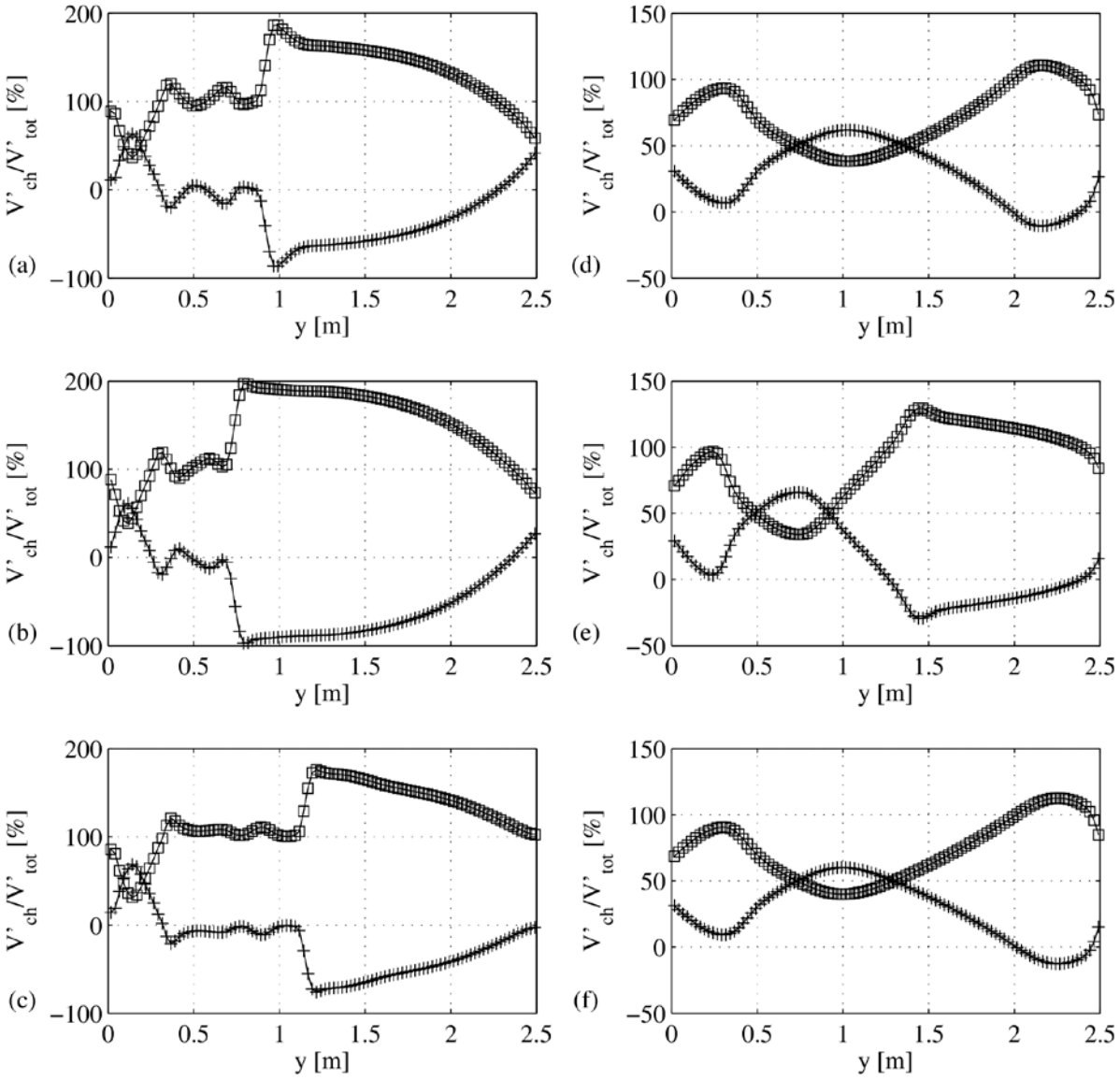

Figure 6 Percentage of total flow rate in the internal (+ signs) and external (□ signs) channels of the façade as a function of height, for cases (a) VL-a, (b) VL-b, (c) VL-c, (d) VH-a, (e) VH-b, (f) VH-c.

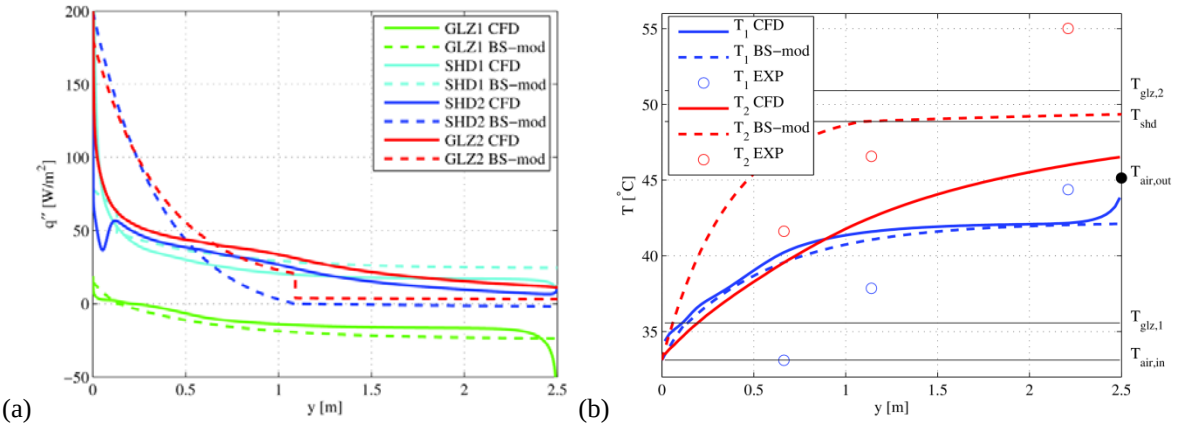

Figure 7 Profiles of wall heat flux (a) and bulk temperature (b) obtained by the BS-model and CFD, case RM-b.

In fact, by observing Figures 4a and 4b, it appears that the main flow initially enters the external channel, only to be dragged towards the internal channel due to the buoyancy induced by the heated blinds. Successively, when the fluid mean temperature exceeds that of the internal glass, recirculation sets on and the main flow re-enters the external channel. Such considerations are well supported by the plots of flow rate distribution of Figure 6: in the VL cases the flow in the internal channel is directed downwards for almost the whole height of the façade, while for higher flow rates (VH cases) the recirculation region is limited to the second half of the façade. Furthermore, both for the VL and VH cases, the point at which the flow rate of the internal channel changes its sign is extremely sensitive to boundary conditions; in particular, the stronger the temperature gradients, the more such point is shifted towards the lower end of the façade.

Finally, Figure 7 reports the profiles of heat flux along all walls, and of the bulk temperature, as calculated by CFD and the BS-model, as a function of height, for a case with roller blinds (RM-b). It can be observed that the two methods match each other fairly well in terms of both heat flux and temperature, in the internal channel. However, the BS-model seems to overestimate the bulk temperature, especially in the first part of the external channel, where local heat flux is also higher. It is also worthy to observe that the point where the heat flux on the internal glazing becomes negative (and, hence, the wall starts to cool down the flow, causing the formation of the recirculation bubble) is captured at the same point by both methods. Figure 7b also includes the experimental values of temperature at selected heights and at the outlet section. The larger degree of discrepancy between such data and theoretical results can be ascribed to the adoption of constant temperature boundary conditions at all walls in the models; in fact, pointwise measurements indicate that, in the real case, temperature is distributed along the height of the glazing and shading devices. Nevertheless, it should be pointed out that the outlet temperature is predicted rather accurately by both models; hence, isolated measurements of temperature in the upper part of the channels (as the ones reported in Figure 7b) could be biased by a wrong shielding of the thermocouple to thermal radiation.

CONCLUSION

In this work, the mechanically aided flow in a ventilated double-skin façade containing shading devices like venetian blinds and roller screens was investigated theoretically, based on a previous experiment carried out at Politecnico di Torino.

Simplified approaches based on 1D modelling and 2D CFD were adopted. Results confirm the adequacy of the methodologies providing an insight on the detail of flow and heat transfer in the system. Overall heat transfer predictions hint at a preliminary validation of the CFD model. Detailed results also confirm the adequacy of the assumptions employed by the BS model for the DSF with roller blinds. Further studies are necessary for a complete assessment of the simplified model under different boundary conditions, especially to address flow recirculation phenomena with Venetian blinds.

ACKNOWLEDGEMENT

The authors warmly thank Prof. Marco Perino at the Dept. of Energy of Politecnico di Torino for kindly providing the experimental dataset of the test facility TWINS used here for the models validation.

REFERENCES

CEN 2005, EN 13363-2 Solar protection devices combined with glazing - Calculation of total solar energy transmittance and light transmittance - Part 2: Detailed calculation method

Angelotti A, Dama A, Mazzarella L, Perino M. 2007. Validazione sperimentale di un modello per facciate a “doppia pelle” in ventilazione meccanica. Proceedings of 62nd National Congress ATI, 2007.Vol. 1, pp. 306-311, Salerno, Italy

Jiru T.E., Haghighat F., Perino M., Zanghirella F., 2006, Zonal modeling of double skin facades, Proceedings of EPIC 2006 AIVC, Vol. 1, pp. 129-134, Lyon, France, 20-22 November

Manz H., 2004. Total solar energy transmittance of glass double facades with free convection, Energy and Buildings, vol. 36, pp. 127-136

Menter FR Two-Equation Eddy-Viscosity Turbulence Models for Engineering Applications, AIAA Journal Vol. 32, no 8. pp. 1598-1605, 1994.

Micono C., Perino M., Serra V., Zanghirella F., Filippi M, 2006, Performance assessment of innovative transparent active envelopes through measurements in test cells, Research in Building Physics and Building Engineering. In Proceedings of 3° Int. Building Physic Conference, Montreal, Quebec, Canada

Park C.S., Augenbroe G., Messadi T, Thitiswat M., Sadegh N., 2004, Calibration of a lumped simulation model for double skin facade system, Energy and Buildings, vol. 36, pp. 1117-1130

Patankar SV Numerical Heat Transfer and Fluid Flow. 1st ed. Hemisphere, Washington DC; 1980.

Saelens D. 2002 Energy Performance Assessment of Single Storey Multiple Skin Facades, PhD Thesis. Leuven (Belgium).

Tanimoto J., Kimura K., 1997, Simulation study on air flow window system with an integrated roll screen, Energy and Buildings, vol. 26, pp. 317-325,

Weller HG, Tabor G, Jasak H, Fureby C. A tensorial approach to computational continuum mechanics using object orientated techniques. Comp. Phys. Vol. 12, pp. 620-631, 1998.

Wilcox DC, Turbulence Modeling for CFD. 3rd ed. DCW Industries; 2006.

Zollner A., Winter E.R.F. Viskanta R, 2002, Experimental studies of combined heat transfer in turbulent mixed convection fluid flows in double skin facades, Int. Journal of Heat and Mass Transfer, vol. 45, pp. 4401-4408,